Scientia Pharmaceutica

ÖSTERREICHISCHE PHARMAZEUTISCHE GESELLSCHAFT

MDPI

Article

New Quinazolin-4(3*H*)-one Derivatives Incorporating Hydrazone and Pyrazole Scaffolds as Antimicrobial Agents Targeting DNA Gyraze Enzyme

Eman M. Mohi El-Deen [1,*], Eman S. Nossier [2] and Eman A. Karam [3]

[1] Department of Therapeutic Chemistry, National Research Centre, Dokki, Cairo 12622, Egypt
[2] Department of Pharmaceutical Medicinal Chemistry, Faculty of Pharmacy (Girls), Al-Azhar University, Cairo 11754, Egypt
[3] Department of Microbial Chemistry, National Research Centre, Dokki, Cairo 12622, Egypt
* Correspondence: e.mohi.2010@live.com; Tel.: +20-0106-385-3338

Abstract: The present work includes the synthesis of a new series of quinazolin-4(3*H*)-one compounds (**4a–f**, **5a–d**) as antimicrobial agents. The starting compound, 2-hydrazinylquinazolin-4(3*H*)-one (**2**), was synthesized and treated with different carbonyl compounds to afford the hydrazone derivatives **4a–f**. In addition, the hydrazone derivatives **4a–d** were treated with a DMF/$POCl_3$ mixture to give the formyl-pyrazole derivatives **5a–d**. All the target compounds were evaluated as antimicrobial agents against four bacterial and four fungal strains. The majority of the tested compounds showed potent antimicrobial activity compared with the reference antibiotics. The most potent antimicrobial activity was shown by **5a** with MIC values in the range (1–16) μg/mL. In addition, the most potent compounds against *E. coli* were evaluated for their inhibitory activity against *E. coli* DNA gyrase, whereas the target compounds **4a**, **5a**, **5c**, and **5d** showed the most potent inhibition to the target enzyme with IC_{50} values ranging from 3.19 to 4.17 μM. Furthermore, molecular docking studies were performed for the most active compounds against the target *E. coli* DNA gyrase to determine their binding affinity within the enzyme's active site. Moreover, ADME evaluations of these compounds predicted their high oral bioavailability and good GI absorption.

Keywords: quinazolin-4(3*H*)-ones; hydrazones; 4-formylpyrazoles; antimicrobial evaluation; DNA gyrase inhibitors; molecular docking; ADME studies

Citation: Mohi El-Deen, E.M.; Nossier, E.S.; Karam, E.A. New Quinazolin-4(3*H*)-one Derivatives Incorporating Hydrazone and Pyrazole Scaffolds as Antimicrobial Agents Targeting DNA Gyraze Enzyme. *Sci. Pharm.* **2022**, *90*, 52. https://doi.org/10.3390/scipharm90030052

Academic Editor: William A. Donaldson

Received: 2 August 2022
Accepted: 17 August 2022
Published: 26 August 2022

1. Introduction

In the last few decades, the risk of infectious diseases has emerged as a growing threat to global health [1], where severe infections of several resistant bacterial strains have become very common, which have shown a diverse resistance pattern to many commonly used antibiotics [2,3]. Thus, the risk of antimicrobial resistance has led to the pressing need to discover new antimicrobial molecules having structural features different from those of the present antibiotics to defeat the resistance mechanisms [4]. Most clinically significant antibiotics such as β-lactams, quinolones, carbapenems, and aminoglycosides have a specific mode of action as microbial enzyme inhibitors; they target specifically the enzymes that are responsible of vital functions such as the biosynthesis of the cell wall, proteins, nucleic acids, and metabolites [5,6]. However after decades of using these antibiotics, their binding to the target enzymes has been obstructed by different resistance mechanisms [7]. Among these enzymes, DNA gyrase, which is present in all microbial cells, plays a pivotal role in bacterial cell cycle progression by introducing negative supercoils into DNA during replication [8,9]. As a result, DNA gyrase inhibition leads to cell death and prevents resistance development [10].

On the other hand, quinazolin-4(3*H*)-one compounds have attracted great interest due to their significant pharmacological activities, including anticancer [11–13], antimi-

crobial [14–16], anti-inflammatory [17,18], analgesic [19,20], antimalarial [21,22], and antiviral [23] activities. Moreover, several quinazolinone derivatives have been reported as potential antimicrobial agents and DNA gyrase inhibitors I–III (Figure 1) [24–26].

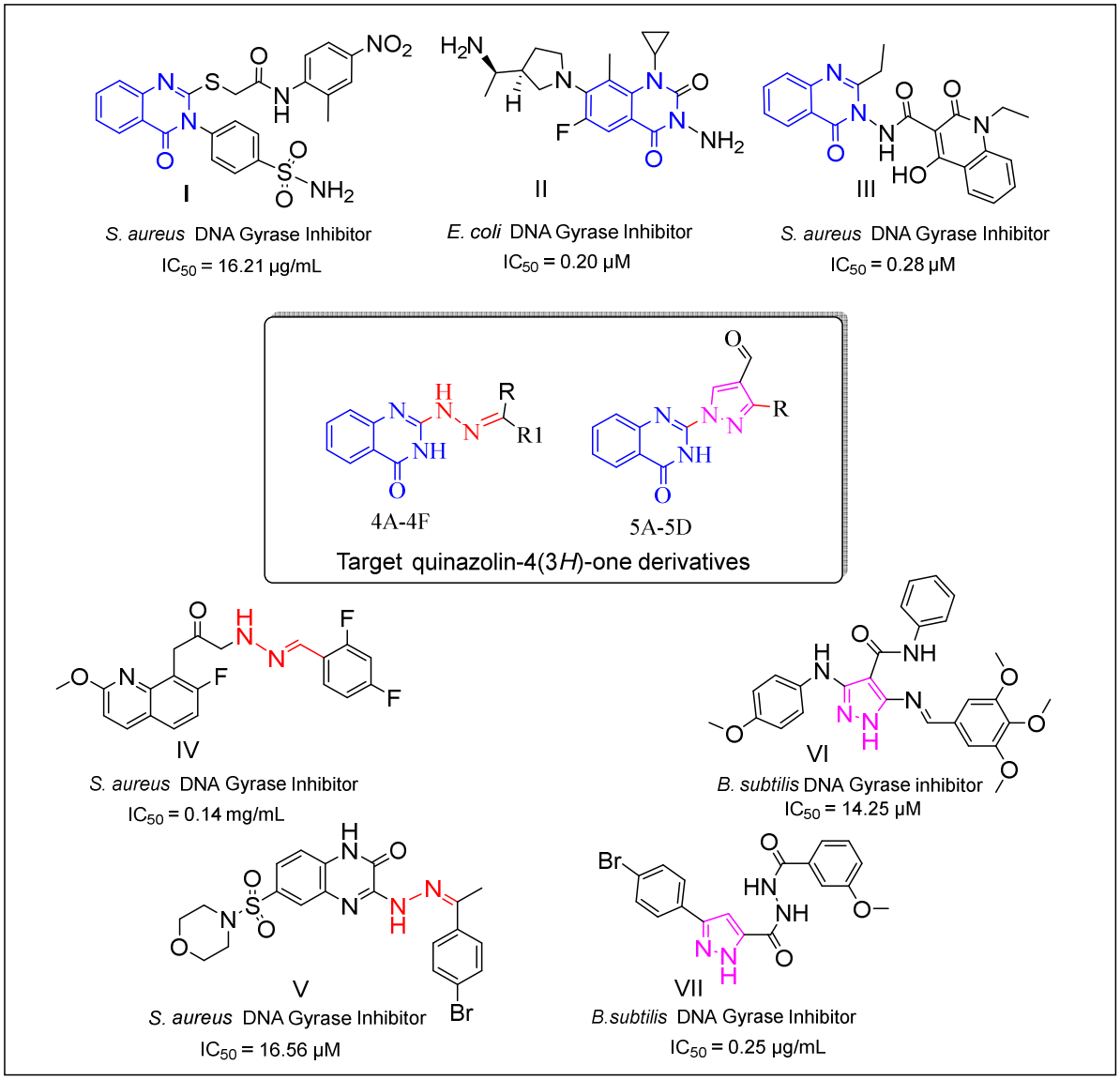

Figure 1. Reported quinazolin-4(3*H*)one derivatives (I-III), hydrazone derivatives (IV,V), and pyrazole compounds (VI,VII) as antimicrobial agents targeting DNA gyrase and the design of the target compounds.

In addition, hydrazones and pyrazole derivatives have received renewed interest due to their various important biological activities [27–30], and some recent studies have explored novel compounds carrying hydrazone and pyrazole moieties as promising candidates to be potent DNA gyrase inhibitors IV–VII (Figure 1) [31–34].

Molecular hybridization is an important concept in drug design; it is based on the combination of different pharmacophores to produce innovative hybrid compounds with improved bioactive efficacy and is considered as one of the recent strategies used for developing new antimicrobial agents to overcome resistance mechanisms [35].

In view of the above topics, the present work includes the design and synthesis of novel hybrid compounds having a quinazolin-4(3*H*)-one nucleus combined with hydrazone or 4-formylpyrazole moieties (**4a**–**4f**, **5a**–**5d**) to obtain potent antimicrobial agents targeting the DNA gyrase enzyme. The in vitro antimicrobial activities of the target compounds were

evaluated against four bacterial and four fungal strains. Molecular docking investigations were also performed for the target compounds against *E. coli* DNA gyrase to determine the binding affinity of the compounds and their binding style within the enzyme's active site.

2. Materials and Methods

2.1. Chemistry

2.1.1. General Information

All melting points were uncorrected and were taken in open capillary tubes using an Electro thermal IA9100 digital melting point apparatus. Elemental microanalyses were carried out at the Micro Analytical Unit at Cairo University. The ESI-mass spectra were measured using an Advion Compact Mass Spectrometer (CMS) NY (New York), USA. Infrared spectra were recorded at the National Research Centre, by using the KBr disc technique on a Jasco FT/IR-360 plus Infrared spectrometer in the range (400–4000 cm^{-1}), made in Japan. ^{1}H NMR and ^{13}C NMR spectra were recorded on a JEOL (Tokyo, Japan) High Performance Digital FT-NMR S (500/125 MHz) in the presence of TMS as the internal standard. The follow-up of the reactions and checking the purity of the compounds were performed by TLC on silica-gel-precoated aluminum sheets (Type 60, F 254, Merck, Darmstadt, Germany) using chloroform/methanol (3:1, *v*/*v*), and the spots were detected by exposure to a UV lamp at δ 254 nanometers for a few seconds and by iodine vapor. The chemical names given for the synthesized compounds were according to the IUPAC system. The starting compound 2-thioxo-2,3-dihydroquinazolin-4(1*H*)-one was prepared by the reported method [36].

2.1.2. Synthesis of 2-hydrazinylquinazolin-4(3*H*)-one (**2**)

A mixture of compound **1** (8.91 g, 0.05 mol) and hydrazine hydrate 100% (4 mL) in absolute ethanol (50 mL) was refluxed for 12 h. The excess solvent was evaporated till dryness under a vacuum. Then, the obtained solid was treated with cold water, collected by filtration, and recrystallized from ethanol to give compound **2**.

Yield 72%, white powder, m.p. 361–362 °C (Lit. m.p. 355 °C [37]); IR (KBr, υ_{max}/cm^{-1}): 3431, 3308, 3187 (NH), 3036 (CH-aromatic), 1674 (C=O), 1601 (C=N). ^{1}H NMR (500 MHz, DMSO-d_6, δ ppm): 7.13 (d, 1H, *J* = 7.6 Hz, Ar-H), 7.42 (d, 1H, *J* = 8.6 Hz, Ar-H), 7.63–7.81 (m, 2H, Ar-H), 8.09 (s, 2H, NH_2, D_2O exchangeable), 8.12, 10.24 (2 s, 2H, 2NH, D_2O exchangeable). ^{13}C NMR (125 MHz, DMSO-d_6, δ ppm): 122.95, 126.83, 127.02, 127.38, 134.52, 146.44, 154.83 (Ar-C, C=N), 163.91(C=O). Anal. Calcd. for $C_8H_8N_4O$ (176.18): C, 54.54; H, 4.58; N, 31.80%; Found: C, 54.78; H, 4.86; N, 31.55%. ESI-MS: *m*/*z* = 175.13 [M-H^+].

2.1.3. Synthesis of 2-(2-ethylidene-hydrazinyl)quinazolin-4(3H)-one Derivatives 4a–f

A mixture of the 2-hydrazinyl derivative **2** (0.88 g, 5 mmol) and the appropriate carbonyl compound **3a**–**f** (5 mmol) in glacial acetic acid (20 mL) was refluxed for 6 h. The mixture was poured onto an ice water mixture, and the obtained solid was collected by filtration and recrystallized from acetone to give the corresponding target compound **4a**–**f**.

2-(2-(1-(Furan-2-yl)ethylidene)hydrazinyl)quinazolin-4(3*H*)-one (**4a**)

Yield 74%, light beige powder, m.p. 220–221 °C. IR (KBr, υ_{max}/cm^{-1}): 3420, 3114 (NH), 3041 (CH-aromatic), 2919, 2851 (CH-aliphatic), 1683 (C=O), 1618, 1579 (C=N). ^{1}H NMR (500 MHz, DMSO-d_6, δ ppm): 2.24 (s, 3H, N=C–CH_3), 6.56 (d, 1H, *J* = 8.6 Hz, Ar-H), 7.09–7.21 (m, 2H, Ar-H), 7.42 (d, 1H, *J* = 8.6 Hz, Ar-H), 7.59–7.70 (m, 2H, Ar-H), 7.84 (d, 1H, *J* = 7.6 Hz, Ar-H), 10.35, 11.18 (2 s, 2H, 2NH, D_2O exchangeable). ^{13}C NMR (125 MHz, DMSO-d_6, δ ppm): 16.90 (CH_3), 110.21, 110.66, 122.89, 126.93, 127.49, 127.74, 134.42, 139.98, 140.45, 146.73, 155.02, 156.79 (Ar-C, 2C=N), 162.18 (C=O). Anal. Calcd. for $C_{14}H_{12}N_4O_2$ (268.28): C, 62.68; H, 4.51; N, 20.88%; Found: C, 62.94; H, 4.25; N, 21.09%. ESI–MS: *m*/*z* = 267.31 [M-H^+].

2-(2-(1-(Thiophen-2-yl)ethylidene)hydrazinyl)quinazolin-4(3*H*)-one (**4b**)

Yield 71%, brown powder, m.p. 278 °C. IR (KBr, υ_{max}/cm^{-1}): 3452, 3164 (NH), 3044 (CH-aromatic), 2919, 2858 (CH-aliphatic), 1680 (C=O), 1630, 1582 (C=N). ^{1}H NMR (500 MHz, DMSO-d_6, δ ppm): 2.36 (s, 3H, N=C–CH_3), 7.06 (d, 1H, *J* = 7.2 Hz, Ar-H), 7.14 (d, 1H, *J* = 7.5 Hz, Ar-H), 7.42–7.51 (m, 2H, Ar-H), 7.67–7.72 (m, 2H, Ar-H), 7.85 (d, 1H, *J* = 7.7 Hz, Ar-H), 10.29, 11.09 (2 s, 2H, 2NH, D_2O exchangeable). ^{13}C NMR (125 MHz, DMSO-d_6, δ ppm): 15.12 (CH_3), 121.11, 122.68, 124.55, 125.03, 127.08, 127.40, 134.38, 140.03, 141.01, 146.87, 155.18, 156.71 (Ar-C, 2C=N), 161.90 (C=O). Anal. Calcd. for $C_{14}H_{12}N_4OS$ (284.34): C, 59.14; H, 4.25; N, 19.70; S, 11.28%; Found: C, 59.42; H, 4.58; N, 19.98; S, 10.97%. ESI–MS: *m*/*z* = 283.27 [M-H$^+$].

2-(2-(1-(Pyridin-2-yl)ethylidene)hydrazinyl)quinazolin-4(3*H*)-one (**4c**)

Yield 78%, pale yellow powder, m.p. 213–214 °C. IR (KBr, υ_{max}/cm^{-1}): 3432, 3158 (NH), 3063 (CH-aromatic), 2919, 2852 (CH-aliphatic), 1689 (C=O), 1622, 1589 (C=N). ^{1}H NMR (500 MHz, DMSO-d_6, δ ppm): 2.40 (s, 3H, N=C–CH_3), 7.12 (d, 1H, *J* = 7.6 Hz, Ar-H), 7.27–7.32 (m, 2H, Ar-H), 7.48–7.59 (m, 2H, Ar-H), 7.76–7.87 (m, 2H, Ar-H), 8.53 (d, 1H, *J* = 6.5 Hz, Ar-H), 10.46, 11.11 (2 s, 2H, 2NH, D_2O exchangeable).^{13}C NMR (125 MHz, DMSO-d_6, δ ppm): 13.16 (CH_3), 122.76, 123.97, 124.92, 126.91, 127.35, 127.85, 135.77, 136.55, 145.12, 148.79, 149.97, 153.73, 155.95 (Ar-C, 2C=N), 161.59 (C=O). Anal. Calcd. for $C_{15}H_{13}N_5O$ (279.30): C, 64.51; H, 4.69; N, 25.07%; Found: C, 64.79; H, 4.85; N, 24.88%. ESI–MS: *m*/*z* = 278.27 [M-H$^+$].

2-(2-(1-(4-Methoxyphenyl)ethylidene)hydrazinyl)quinazolin-4(3*H*)-one (**4d**)

Yield 69%, greenish yellow powder, m.p. 287–288 °C. IR (KBr, υ_{max}/cm^{-1}): 3425, 3191 (NH), 3056 (CH-aromatic), 2919, 2849 (CH-aliphatic), 1694 (C=O), 1638, 1591 (C=N). ^{1}H NMR (500 MHz, DMSO-d_6, δ ppm): 2.33 (s, 3H, N=C–CH_3), 3.77 (s, 3H, OCH_3), 7.14 (d, 1H, *J* = 7.6 Hz, Ar-H), 7.30 (d, 2H, *J* = 8.2 Hz, Ar-H), 7.44 (d, 1H, *J* = 8.6 Hz, Ar-H), 7.59–7.62 (m, 1H, Ar-H), 7.83 (d, 1H, *J* = 7.6 Hz, Ar-H), 8.11 (d, 2H, *J* = 8.2 Hz, Ar-H), 10.34, 11.22 (2 s, 2H, 2NH, D_2O exchangeable). ^{13}C NMR (125 MHz, DMSO-d_6, δ ppm): 16.21 (CH_3), 55.78 (OCH_3), 114.54, 122.89, 126.87, 127.22, 127.56, 127.99, 129.23, 134.54, 146.90, 147.76, 155.01, 160.44 (Ar-C, 2C=N), 161.97 (C=O). Anal. Calcd. for $C_{17}H_{16}N_4O_2$ (308.34): C, 66.22; H, 5.23; N, 18.17%; Found: C, 66.43; H, 5.41; N, 17.92%. ESI–MS: *m*/*z* = 307.39 [M-H$^+$].

2-(2-(4-Methylcyclohexylidene)hydrazinyl)quinazolin-4(3*H*)-one (**4e**)

Yield 76%, orange powder, m.p. 133 °C. IR (KBr, υ_{max}/cm^{-1}): 3422, 3192 (2NH), 3036 (CH-aromatic), 2923, 2861 (CH-aliphatic), 1676 (C=O), 1638, 1598 (C=N). ^{1}H NMR (500 MHz, DMSO-d_6, δ ppm): 0.88 (d, 3H, *J* = 6.7 Hz, CH-C$\underline{H}_3$), 1.21–1.25 (m, 1H, C$\underline{H}$-CH_3), 1.40–2.05 (m, 8H, 4CH_2), 7.12 (d, 1H, *J* = 7.6 Hz, Ar-H), 7.42 (d, 1H, *J* = 8.6 Hz, Ar-H), 7.62 (d, 1H, *J* = 8.95 Hz, Ar-H), 7.82 (d, 1H, *J* = 8.5 Hz, Ar-H), 10.45, 11.21 (2 s, 2H, 2NH, D_2O exchangeable). ^{13}C NMR (125 MHz, DMSO-d_6, δ ppm): 21.75 (CH_3), 26.78, 31.21, 32.10, 35.55 (4CH_2, CH), 122.84, 126.87, 127.03, 127.39, 134.53, 146.60 (Ar-C) 154.45, 161.28, 162.77 (2 C=N, C=O). Anal. Calcd. for $C_{15}H_{18}N_4O$ (270.34): C, 66.64; H, 6.71; N 20.73%; Found: C, 66.47; H, 6.44; N, 20.49%. ESI−MS: *m*/*z* = 269.48 [M-H$^+$].

2-(2-(2-Oxoindolin-3-ylidene)hydrazinyl)quinazolin-4(3*H*)-one (**4f**)

Yield 79%, yellow powder, m.p. 304 °C. IR (KBr, υ_{max}/cm^{-1}): 3432, 3201 (NH), 3062 (CH-aromatic), 1699, 1671 (C=O), 1633, 1596 (C=N). ^{1}H NMR (500 MHz, DMSO-d_6, δ ppm): 7.09 (d, 1H, *J* = 7.6 Hz, Ar-H), 7.29–7.36 (m, 1H, Ar-H), 7.40–7.48 (m, 2H, Ar-H), 7.54–7.81 (m, 3H, Ar-H), 7.91(d, 1H, *J* = 7.6 Hz, Ar-H), 10.50, 10.91, 11.22 (3 s, 3H, 3NH, D_2O exchangeable). ^{13}C NMR (125 MHz, DMSO-d_6, δ ppm): 118.02, 119.35, 122.95, 124.72, 126.83, 127.12, 127.36, 128.61, 130.35, 134.52, 136.64, 140.95, 146.36, 154.73 (Ar-C, 2C=N), 161.97, 169.03 (2 C=O) Anal. Calcd. for $C_{16}H_{11}N_5O_2$ (305.30): C, 62.95; H, 3.63; N, 22.94%; Found: C, 62.61; H, 3.39; N, 22.66%. ESI−MS: *m*/*z* = 304.24 [M-H$^+$].

2.1.4. Synthesis of 1-(4-oxo-3,4-dihydroquinazolin-2-yl)-1*H*-pyrazole-4-carbaldehyde Derivatives (**5a**–**d**)

To a cold solution of phosphorus oxychloride (1.2 mL) in *N*,*N*-dimethyl formamide DMF (10 mL) at (0–5) °C, the hydrazone derivatives **4a**–**d** (1 mmol) were added portionwise with stirring. After addition, the cold solution was stirred for 1 h, then heated with stirring at 60–65 °C for 3h. The reaction solution was poured onto an ice–water mixture, and the acidic medium was neutralized by adding a small amount of dilute ammonia solution (10%) The formed solid was collected by filtration and recrystallized from ethanol to give the 4-formyl pyrazole derivatives **5a**–**d**.

3-(Furan-2-yl)-1-(4-oxo-3,4-dihydroquinazolin-2-yl)-1*H*-pyrazole-4-carbaldehyde (**5a**)

Yield 68%, buff powder, m.p. 191–192 °C. IR (KBr, υ_{max}/cm^{-1}): 3434 (NH), 3089 (CH-aromatic), 1680 (C=O), 1628 (C=N). ^{1}H NMR (500 MHz, DMSO-d_6, δ ppm): 6.67 (s, 1H, Ar-H), 7.12 (d, 1H, *J* = 7.6 Hz, Ar-H), 7.46–7.64 (m, 3H, Ar-H), 7.79–7.83 (m, 2H, Ar-H), 8.12 (s, 1H, CH-pyrazole), 9.68 (s, 1H, H–C=O), 10.11 (s, 1H, NH, D_2O exchangeable). ^{13}C NMR (125 MHz, DMSO-d_6, δ ppm): 112.47, 113.65, 115.35, 122.77, 126.88, 127.20, 127.40, 135.52, 135.81, 136.82, 144.14, 145.31, 145.98, 153.04 (Ar-C, C=N) 162.69, 185.42 (2C=O). Anal. Calcd. for $C_{16}H_{10}N_4O_3$ (306.28): C, 62.74; H, 3.29; N, 18.29%; Found: C, 62.53; H, 3.14; N, 17.98%. ESI−MS: m/z = 305.22 [M-H$^+$].

1-(4-Oxo-3,4-dihydroquinazolin-2-yl)-3-(thiophen-2-yl)-1*H*-pyrazole-4-carbaldehyde (**5b**)

Yield 67%, pale grey powder, m.p. 224 °C. IR (KBr, υ_{max}/cm^{-1}): 3441 (NH), 3098 (CH-aromatic), 1687 (C=O), 1617 (C=N). ^{1}H NMR (500 MHz, DMSO-d_6, δ ppm): 7.15 (d, 1H, *J* = 7.6 Hz, Ar-H), 7.42 (d, 1H, *J* = 8.6 Hz, Ar-H), 7.64–7.70 (m, 3H, Ar-H), 7.82 (d, 1H, *J* = 7.6 Hz, Ar-H), 8.10 (d, 1H, *J* = 7.7 Hz, Ar-H), 8.24 (s, 1H, CH-pyrazole) 9.44 (s, 1H, H–C=O), 10.07 (s, 1H, NH, D_2O exchangeable). ^{13}C NMR (125 MHz, DMSO-d_6, δ ppm): 115.87, 122.90, 126.94, 127.19, 127.52, 127.99, 128.58, 129.55, 130.72, 133.15, 135.58, 139.12, 143.75, 153.49 (Ar-C, C=N) 162.49, 185.48 (2C=O). Anal. Calcd. for $C_{16}H_{10}N_4O_2S$ (322.34): C, 59.62; H, 3.13; N, 17.38; S, 9.95%; Found: C, 59.87; H, 3.31; N, 17.16; S, 10.18%. ESI−MS: m/z = 321.37 [M-H$^+$].

1-(4-Oxo-3,4-dihydroquinazolin-2-yl)-3-(pyridin-2-yl)-1*H*-pyrazole-4-carbaldehyde (**5c**)

Yield 64%, dark brown powder, m.p. 178 °C. IR (KBr, υ_{max}/cm^{-1}): 3404 (2NH), 3084 (CH-aromatic), 1697 (C=O), 1627 (C=N). ^{1}H NMR (500 MHz, DMSO-d_6, δ ppm): 7.12 (d, 1H, *J* = 7.6 Hz, Ar-H), 7.30–7.51 (m, 3H, Ar-H), 7.63–7.69 (m, 2H, Ar-H), 7.83 (d, 1H, *J* = 7.7 Hz, Ar-H), 8.21 (s, 1H, CH-pyrazole), 8.48 (d, 1H, *J* = 6.5 Hz, Ar-H) 9.53 (s, 1H, H–C=O), 10.15 (s, 1H, NH, D_2O exchangeable). ^{13}C NMR (125 MHz, DMSO-d_6, δ ppm): 115.59, 122.85, 123.08, 125.21, 126.97, 127.09, 127.69, 135.10, 135.58, 136.77, 138.01, 146.54, 149.78, 153.50, 156.12 (Ar-C, C=N) 162.51, 185.39 (2C=O). Anal. Calcd. for $C_{17}H_{11}N_5O_2$ (317.31): C, 64.35; H, 3.49; N, 22.07%; Found: C, 64.58; H, 3.68; N, 22.29%. ESI−MS: m/z = 316.27 [M-H$^+$].

3-(4-Methoxyphenyl)-1-(4-oxo-3,4-dihydroquinazolin-2-yl)-1*H*-pyrazole-4-carbaldehyde (**5d**)

Yield 67%, brown, m.p. 163–164 °C. IR (KBr, υ_{max}/cm^{-1}): 3408 (NH), 3087 (CH-aromatic), 2918 (CH-aliphatic), 1696 (C=O), 1619 (C=N). ^{1}H NMR (500 MHz, DMSO-d_6, δ ppm): 3.82 (s, 3H, OCH_3), 7.13–7.25 (m, 3H, Ar-H), 7.42 (d, 1H, *J* = 8.6 Hz, Ar-H), 7.61–8.06 (m, 4H, Ar-H), 8.17 (s, 1H, CH-pyrazole), 9.69 (s, 1H, H–C=O), 10.06 (s, 1H, NH, D_2O exchangeable). ^{13}C NMR (125 MHz, DMSO-d_6, δ ppm): 56.09 (OCH_3), 112.08, 114.87, 122.91, 124.98, 126.94, 127.44, 127.65, 128.08, 129.42, 134.49, 137.33, 146.87, 153.12, 160.29 (Ar-C, C=N), 162.07, 185.31 (2C=O). Anal. Calcd. for $C_{19}H_{14}N_4O_3$ (346.35): C, 65.89; H, 4.07; N, 16.18%; Found: C, 65.68; H, 4.30; N, 16.47%. ESI−MS: m/z = 345.38 [M-H$^+$].

2.2. Antimicrobial Screening

All the synthesized quinazolin-4(3*H*)-one compounds (**2**, **4a**–**f**, **5a**–**d**) were screened for their in vitro antibacterial activity against four bacterial strains (*Bacillus subtilis* 6633,

Staphylococcus aureus 25923, *Salmonella typhimurium* 14028, and *Escherichia coli* 8739) compared with Amoxicillin trihydrate as the reference drug. Furthermore, all the compounds were evaluated as antifungal agents against four fungal strains (*Candida tropicals* 750, *Candida albicans* 10231, *Macrophomina phaseolina* A62743, and *Aspergillus niger* EM77 KF774181) compared with the reference drug Clotrimazole. The diameter of inhibition zone (DIZ) assay was performed by the agar disk diffusion method [38]. The Minimum Inhibitory Concentration (MIC) of the compounds was then evaluated against bacterial strains and fungal strains using the broth dilution method [39]. (More details are provided in the Supplementary Materials S33).

2.3. DNA Gyrase Supercoiling Inhibition Assay

The assay for determining the DNA gyrase supercoiling inhibition for the target compounds (**4a**, **4b**, **4c**, **5a**, **5b**, **5c**, and **5d**) with Novobiocin as a reference inhibitor was performed according to the protocol obtained from the supplier by using the *E. coli* DNA gyrase kit provided by TopoGEN, Inc. (Port Orange, FL, USA) [40–42]. The new compounds and the standard inhibitor were dissolved in DMSO and serially diluted at concentrations of 100, 10, 1, and 0.1 μM, then assayed in reaction mixtures in three different replicate runs. The average IC_{50} values (μM) of the triplicate experiments were calculated for the target compounds and Novobiocin. (More details are provided in the Supplementary Materials S34).

2.4. Molecular Modeling Studies

To investigate the molecular interactions between the most potent quinazolinone derivatives **4a–c** and **5a–d** and the active site of *E. coli* DNA gyrase B kinase, a molecular docking study was performed by using the molecular operating environment ((MOE) software Version 2014.0901, Chemical Computing Group Inc., Montereal, Canada [43]. Then, the geometry optimization and energy minimization were applied to obtain the Conf Search module in MOE, followed by saving the MOE file for the upcoming docking process. The co-crystallized structure of *E. coli* DNA gyrase B kinase with its ligand novobiocin was downloaded (PDB code: 1AJ6) [44]. At first, the validation of the docking process was established by docking of the native ligand, followed by docking of the derivatives **4a–c** and **5a–d** within the ATP-binding site after elimination of co-crystallized ligand. (More details are provided in the Supplementary Materials S35; The 3D binding poses are provided in the Supplementary Materials, Figure S32).

2.5. In Silico ADME Prediction Study

The physicochemical and pharmacokinetic properties of the highly potent quinazolinone compounds **4a**, **5a**, **5c**, and **5d** were predicted by using the free web tool, SwissADME [45–47].

3. Results and Discussion

3.1. Chemistry

The present work included the synthesis of a series of new quinazolin-4(3*H*)one derivatives (**4a–f**, **5a–d**) as illustrated by Schemes 1 and 2. The structure of all synthesized compounds were confirmed by ^{1}H-NMR, ^{13}C-NMR, IR, and mass spectral data (Supplementary Materials, Figures S1–S31), in addition to the correct ratios of their elemental microanalyses. The 2-hydrazinylquinazolin-4(3*H*)-one (**2**) was reported as a key intermediate compound in the synthesis of different quinazolinone-based compounds [48,49]. For the synthesis of the target quinazolinone-hydrazone derivatives, the starting 2-hydrazinyl derivative 2 was synthesized in a good yield by the reaction of 2-thioxo-2,3-dihydroquinazolin-4(1*H*)-one (**1**) with hydrazine hydrate in refluxed ethanol. Upon treatment of the 2-hydrazinyl derivative **2** with different carbonyl compounds (**3a–f**), namely 1-(furan-2-yl)ethan-1-one, 1-(thiophen-2-yl)ethan-1-one, 1-(pyridin-2-yl)ethan-1-one, 1-(4-methoxyphenyl)ethan-1-one, 4-methylcyclohexan-1-one, and indoline-2,3-dione in glacial acetic under reflux, the hydrazone derivatives **4a–f** was afforded (Scheme 1). The IR spectrum of the

2-hydrazinyl derivative **2** showed a strong absorption band at 1674 cm^{-1} related to the C=O group along with three absorption bands at the region 3431–3187 cm^{-1} due to the NH stretching vibration of the NH-quinazolinone and the $–NHNH_2$ moiety. Furthermore, the ^{1}H-NMR spectrum of **2** represented three D_2O exchangeable signals in the range of δ 8.09–10.24 ppm corresponding to the protons of the two NH and the NH_2 groups, besides the signals of the four quinazolinone aromatic protons at their expected regions. Moreover, the ^{13}C-NMR data of the 2-hydrazinyl derivative **2** showed a signal at δ 163.91 ppm related to the C=O group alongside the expected signals of the C=N group and the four aromatic carbons. Moreover, the formation of the hydrazones (**4a**–**f**) was confirmed by their ^{1}H-NMR spectra, which revealed vanishing of the D_2O exchangeable signal of the hydrazide NH_2 group at δ 8.09 ppm of the parent 2-hydrazinyl derivative **2**. In addition, the ^{1}H-NMR spectra of the arylethylidene derivatives (**4a**–**d**) represented the singlet signal corresponding to the CH_3 protons of the $N=C–CH_3$ moiety in the range of δ 2.24–2.40 ppm along with the signals of the new aromatic protons related to the new aryl group. Another support to the structures of (**4a**–**d**) was gained by their ^{13}C-NMR data, which showed signals corresponding to the CH_3 carbon in the range of δ 13.16–16.90 ppm besides the signals of the new aromatic carbons, while the ^{1}H-NMR spectrum of the 4-methylcyclohexylidene derivative **4e** showed the doublet signal at δ 0.88 ppm, the multiplet signal at δ 1.21–1.25 ppm, and the multiplet signal at δ 1.40–2.05 ppm assignable to the protons of CH_3, CH, and $4CH_2$ of the new 4-methylcyclohexylidene moiety, respectively. Furthermore, the ^{13}C-NMR of **4e** assisted in showing the presence of the 4-methylcyclohexylidene carbons by five signals in the range of δ 21.75–35.55 ppm. Moreover, the IR spectrum of the 2-oxoindolin-3-ylidene derivative **4f** exhibited two absorption bands at 1699 and 1671 cm^{-1}, corresponding to the two C=O groups of the indolinone and quinazolinone moieties. Furthermore, the ^{1}H-NMR spectrum of **4f** revealed the signals corresponding to the aromatic protons of the new indolinone moiety alongside three D_2O exchangeable signals assignable to quinazolinone-NH, hydrazone-NH, and the new indolinone-NH in the range of δ 10.50–11.22 ppm. Additionally, the ^{13}C-NMR spectrum of **4f** showed a new signal at δ 169.03 ppm, ascribed to indolinone-C=O, as well as new signals related to the aromatic carbons of the indolinone moiety.

Further treatment of the 2-(2-arylethylidene)hydrazinyl)quinazolin-4(3*H*)-ones **4a**–**f** with the $DMF/POCl_3$ mixture (Vilsmeier–Haack reagent) afforded the 3-aryl-1-(4-oxo-3,4-dihydroquinazolin-2-yl)-1*H*-pyrazole-4-carbaldehydes **5a**–**d** in good yields (Scheme 2), whereas the conversion of the hydrazones **4a**–**d** to the corresponding formyl-pyrazole derivatives **5a**–**d** was achieved via the reported mechanism of the Vilsmeier–Haack reaction [50]. The IR spectra of the formyl-pyrazole derivatives **5a**–**d** showed one strong absorption band in the region 1697–1680 cm^{-1}, corresponding to the two C=O groups of the quinazolinone and the formyl-pyrazole moieties. The ^{1}H-NMR spectra of **5a**–**d** showed only one D_2O exchangeable signal in the range of δ 10.07–10.15 ppm corresponding to quinazolinone-NH with vanishing of the ethylidene-CH_3 signal, which confirmed the formation of the formyl-pyrazole moiety. Moreover, the ^{1}H-NMR spectra of **5a**–**d** revealed, besides the signals of the parent aromatic protons, two new singlet signals at ranges δ 8.12–8.24 ppm and δ 9.44–9.69 ppm, ascribed to CH-pyrazole and the H–C=O protons, respectively. Furthermore, the ^{13}C-NMR spectra **5a**–**d** showed the signals related to all the carbons in the expected regions alongside the signal of the H–C=O carbon in the range of δ 185.31–185.48 ppm. In addition, the molecular structures of the new compounds (**4a**–**f**, **5a**–**d**) were confirmed by their mass spectra, which represent their correct molecular ion peaks.

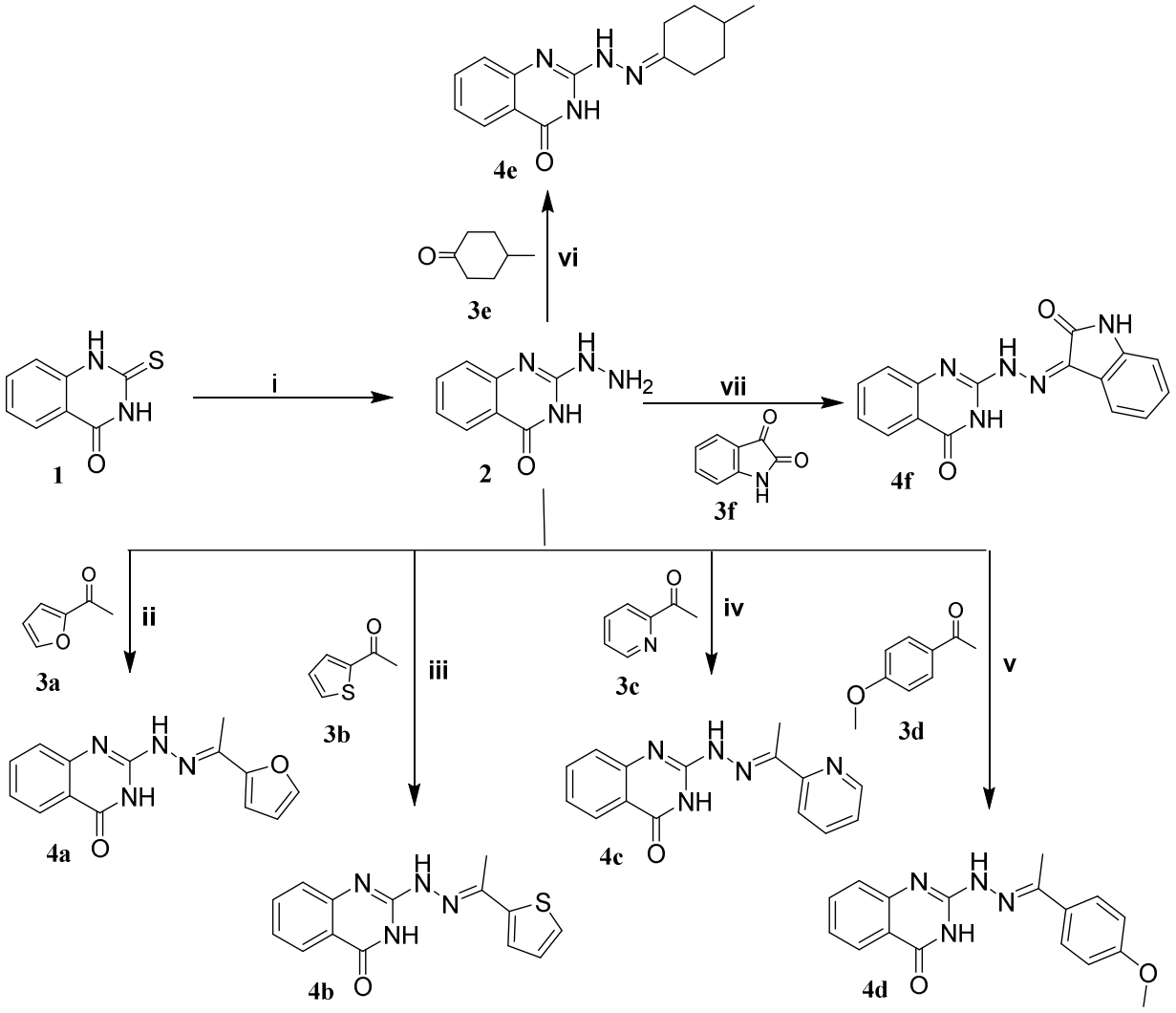

(**i**) Hydrazine hyderate, absolute ethanol, reflux for 12 h; (**ii-vii**) glacial acetic acid, reflux for 6 h..

Scheme 1. Synthesis of new quinazolin-4(3*H*)one derivatives bearing different hydrazone moieties (**4a–f**).

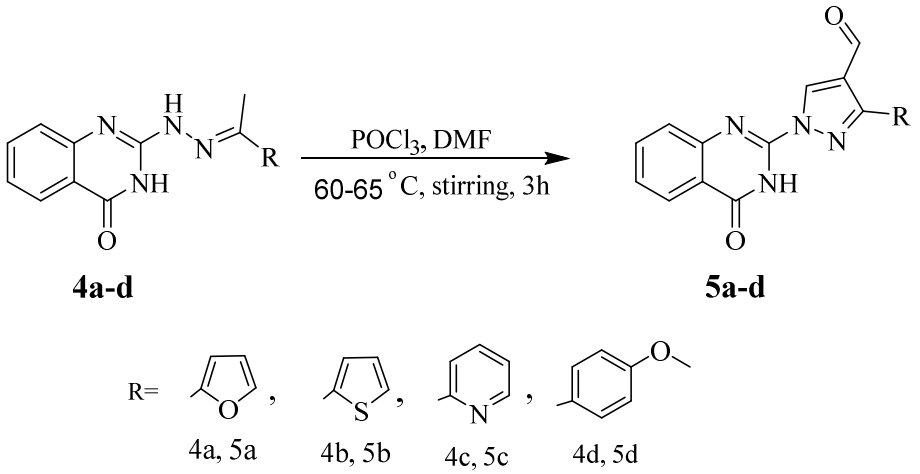

Scheme 2. Synthesis of new quinazolin-4(3*H*)one derivatives bearing 4-formyl-pyrazoles (**5a–d**).

3.2. Antimicrobial Activity

All the synthesized quinazolin-4(3*H*)one derivatives (**2**, **4a**–**f**, **5a**–**d**) were examined as antimicrobial agents against a number of bacterial and fungal strains. The tested microorganisms include two Gram-positive bacteria (*B. subtilis* 6633, *S. aureus* 25923), two Gram-negative bacteria (*S. typhimurium* 14028, *E coli* 8739), two yeast strains (*C. tropicals* 750, *C. albicans* 10231), and two fungal strains (*M. phaseolina* A62743, *A. niger* EM77-KF774181) compared with Amoxicillin trihydrate and Clotrimazole as reference drugs against the bacterial and fungal strains, respectively. The average diameters of the inhibition zones in mm were determined for the target compounds and the reference antibiotics and are listed in Table 1. Then, the MIC values in (μg/mL) were determined and are listed in Table 2 and represented by Figures 2 and 3.

Table 1. In vitro antimicrobial activities of the synthesized quinazolin-4(3*H*)-one derivatives represented as the mean diameter of the inhibition zone in mm.

	Antibacterial Activity				**Antifungal Activity**			
Compd.	***S. aureus***	***B. subtilis***	***E. coli***	***S. typhimurium***	***C. albicans***	***C. tropicals***	***M. phaseolina***	***A. niger***
2	25	22	20	14	20	20	19	19
4a	30	29	30	27	32	25	27	25
4b	26	24	26	26	20	18	16	26
4c	29	28	28	29	30	32	29	30
4d	17	18	20	16	15	14	15	18
4e	24	22	21	22	20	22	22	20
4f	15	17	16	-	-	14	-	17
5a	35	34	35	38	39	35	30	29
5b	26	24	26	26	16	21	20	19
5c	30	30	33	31	27	28	24	22
5d	31	29	34	26	28	29	25	27
Amoxicillin	29	28	28	27	-	-	-	-
Clotrimazole	-	-	-	-	26	25	24	26

Table 2. In vitro antimicrobial activities of the synthesized quinazolin-4(3*H*)-one derivatives as minimum inhibitory concentrations (MIC) in μg/mL.

	Antibacterial Activity				**Antifungal Activity**			
Compd.	***S. aureus***	***B. subtilis***	***E. coli***	***S. typhimurium***	***C. albicans***	***C. tropicals***	***M. phaseolina***	***A. niger***
2	16	32	64	128	32	32	64	32
4a	4	4	4	8	2	8	8	16
4b	8	8	8	8	32	64	128	16
4c	4	8	8	4	2	4	8	4
4d	64	64	64	64	128	128	128	128
4e	16	32	32	16	32	16	16	32
4f	128	64	128	-	-	128	-	64
5a	2	2	1	1	1	2	4	4
5b	4	8	8	8	32	32	32	32
5c	4	4	2	4	8	8	16	16
5d	4	4	2	8	8	8	16	8
Amoxicillin	4	4	8	8	-	-	-	-
Clotrimazole	-	-	-	-	8	8	16	8

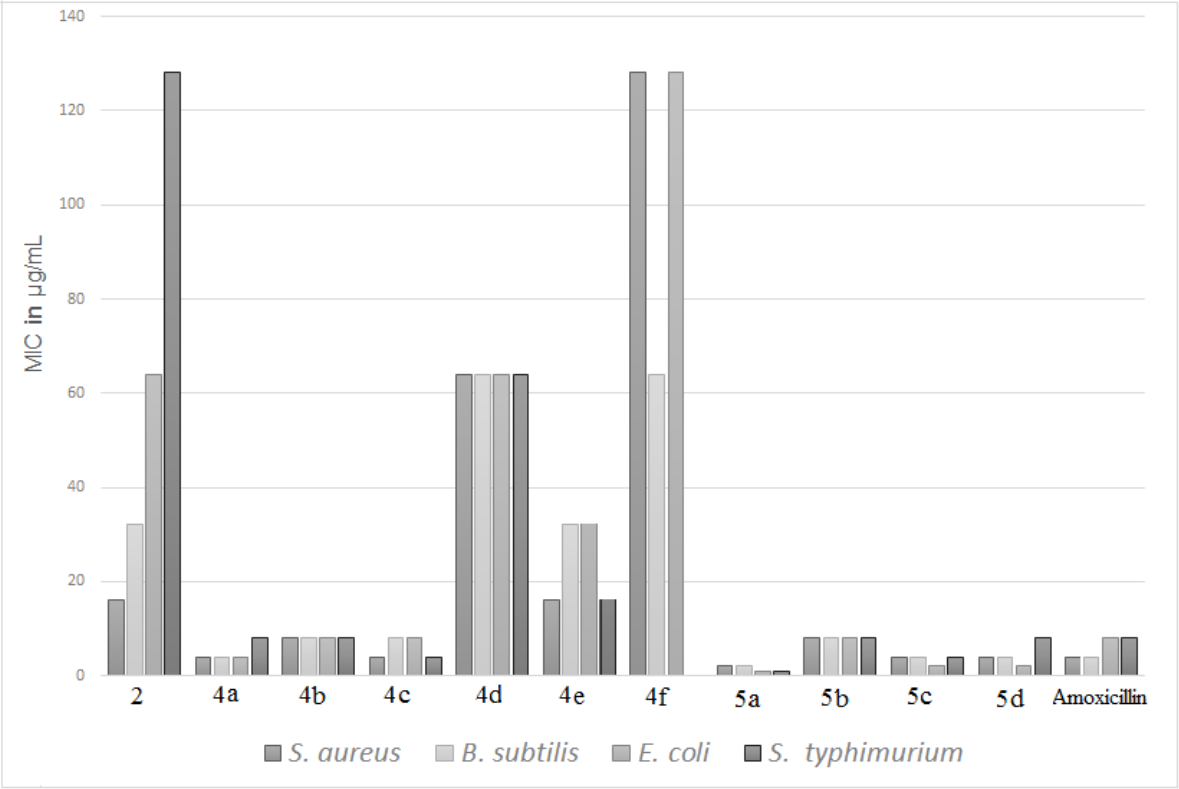

Figure 2. The antibacterial activity (MIC in µg/mL) of the of the synthesized quinazolin-4(3*H*)one derivatives compared with Amoxicillin trihyderate.

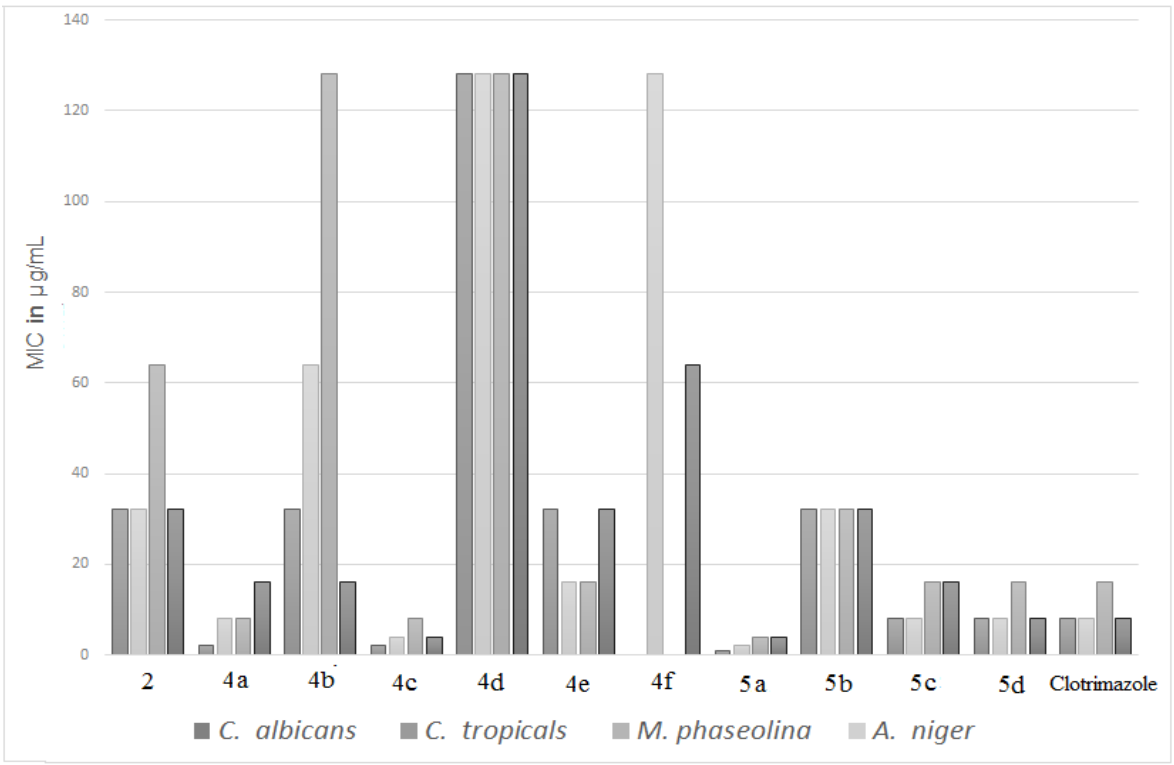

Figure 3. The antifungal activity (MIC in µg/mL) of the synthesized quinazolin-4(3*H*)one derivatives compared with Clotrimazole.

The obtained results of the inhibition zones of the new quinazolin-4(3*H*)-one derivatives (Table 1) revealed that some of the new compounds such as **4a**, **4c**, **5a**, **5c**, and **5d** exhibited large inhibition zones ranging from 22 to 39 mm against bacterial and fungal strains, which indicates the higher sensitivity of the tested strains to the target compounds.

According to the MIC values, it is obvious that the majority of the target compounds showed significant activity against the tested microbial strains. 2-hydrazinylquinazolin-4(3*H*)-one (**2**) revealed antimicrobial activity varying from moderate to weak with MIC values in range of (16–128) μg/mL, while the target hydrazone derivatives (**4a**–**f**) showed a wide variety in their potency against both bacterial and fungal strains, whereas the most potent antibacterial activity was exhibited by the 2-(1-(furan-2-yl)ethylidene derivative **4a**, which exceeded the potency of Amoxicillin against *E. coli* with a MIC value 4 μg/mL ($MIC_{Amoxxicillin}$ = 8 μg/mL) and showed equipotent activity to that of Amoxicillin against *S. aureus, B. subtilis*, and *S. typhimurium* with MIC values of 4, 4, and 8 μg/mL, respectively. Furthermore, **4a** showed potent antifungal activity with MIC values in the range of (2–16) μg/mL, which is more potent than Clotrimazole against *C. albicans* and *M. phaseolina* with MIC values of 2 and 8 μg/mL compared with the MIC values of 8 and 16 μg/mL of Clotrimazole, respectively. Moreover, the 2-(1-(pyridin-2-yl)ethylidene derivative **4c** showed more potent antibacterial activity than Amoxicillin against *S. typhimurium* with a MIC value of 4 μg/mL and showed equipotent activity to that of Amoxicillin against *E. coli* and *S. typhimurium* with a MIC value of 8 μg/mL. Additionally, the antifungal activity of **4c** was the most potent between the target hydrazones with MIC values in the range of (2–8) μg/mL, which exceeded the antifungal activity of Clotrimazole against the four tested strains. The activity of the 2-(1-(thiophen-2-yl)ethylidene derivative **4b** came after **4a** and **4c** against bacterial strains; it showed similar sensitivity towards the four tested strains with a MIC value of 8 μg/mL. However, it revealed lower antifungal activity with MIC values in the range of (16–128) μg/mL. Furthermore, the 2-(4-methylcyclohexylidene derivative **4e** showed moderate activity against the tested microorganisms with MIC values varying from 16 to 32 μg/mL. An apparent decrease of the antimicrobial activity was shown by the 2-(1-(4-methoxyphenyl)ethylidene derivative **4d** and 2-oxoindolin-3-ylidene derivative **4f**; they revealed weak or no activity against the tested bacterial and fungal strains.

In addition, the conversion of the hydrazone derivatives **4a**–**d** to the formyl-pyrazole derivatives **5a**–**d** led to an obvious increase in the antimicrobial activity, especially against the bacterial strains, whereas the 3-(furan-2-yl)-1*H*-pyrazole-4-carbaldehyde derivative **5a** exhibited the most potent antimicrobial activity among the tested compounds and the reference drugs with MIC values in the range of (1–4) μg/mL. Moreover, the 3-(thiophen-2-yl)-1*H*-pyrazole-4-carbaldehyde **5b** showed similar antibacterial activity to that of Amoxicillin against three of the tested bacterial strains and showed moderate antifungal activity against the four fungal strains with the same MIC value = 32 μg/mL. In addition, the 3-(pyridin-2-yl)-1*H*-pyrazole-4-carbaldehyde derivative **5c** displayed more potent activity than that of Amoxicilli against *E. coli* and *S. typhimurium* with MIC values of 2 and 4 μg/mL, respectively, while it showed some decrease in the activity against the four tested fungal strains, compared with its parent hydrazone derivative **4c**, with MIC values in the range of (8–16) μg/mL. Finally, the 3-(4-methoxyphenyl)-1*H*-pyrazole-4-carbaldehyde **5d** showed much higher potency against both the tested bacterial and fungal strains compared with **4d**. It revealed more potent activity than Amoxicillin against *E. coli* and equal potency to the reference drugs against the other tested microorganisms.

3.3. In Vitro DNA Gyrase Inhibitory Activity

The target compounds of the most potent antibacterial activity (**4a**, **4b**, **4c**, **5a**, **5b**, **5c**, and **5d**) were subjected to further screening for their inhibition profiles against *E coli* DNA gyrase compared with Novobiocin as a reference DNA gyrase inhibitor. The results of the IC_{50} values of the tested compounds in Table 3 showed that the most potent inhibitory activity was exhibited by the 3-(furan-2-yl)-1*H*-pyrazole-4-carbaldehyde derivative **5a** with an IC_{50} value of 3.19 μM and the 3-(4-methoxyphenyl)-1*H*-pyrazole-4-carbaldehyde **5d** with

an IC_{50} value of 3.51 μM, which exceeded the inhibition potency of Novobiocin with an IC_{50} value of 4.12 μM. Furthermore, the 3-(pyridin-2-yl)-1*H*-pyrazole-4-carbaldehyde derivative **5c** and the 2-(1-(furan-2-yl)ethylidene derivative **4a** showed potent inhibition with IC_{50} values of 4.09 and 4,17 μM, respectively, which were nearly equal to that of the reference inhibitor, while the other target compounds **4b**, **4c**, and **5b** revealed lower inhibition potency against the target enzyme with IC_{50} values in the range of (10.82–16.91) μM.

Table 3. In vitro enzymatic inhibitory activity against *E coli* DNA gyrase.

Compound No.	DNA Gyrase Supercoiling Inhibition IC_{50} (μM)
4a	4.17 ± 0.07
4b	16.91 ± 0.36
4c	15.08 ± 0.34
5a	3.19 ± 0.06
5b	10.82 ± 0.24
5c	4.09 ± 0.13
5d	3.51 ± 0.10
Novobiocin	4.12 ± 0.11

3.4. Molecular Docking Study on E. coli DNA Gyrase B Kinase

The docking simulation of the most active novel quinazolin-4(3*H*)one derivatives (**4a–c**, **5a–d**) was established in an attempt to explain their variable gained potencies with *E. coli* DNA gyrase B kinase. The process of molecular docking was firstly validated through self-docking of the co-crystallized ligand Novobiocin within the active site of *E. coli* DNA gyrase B (PDB code: 1AJ6), giving an energy score of −10.25 kcal/mol with small RMSD values of 0.87 Å between the native ligand and its docked pose. The docking results are inserted in Table 4 and revealed that the derivatives **4a–c** and **5a–d** occupied the same binding site through two types of interactions: one was arene–cation interactions between the quinazolinone moiety and **Ile78,** and the other was between the oxygen of the quinazolinone and **Gly77**, whereas the highest binding affinity was revealed by the target compounds **4a**, **5a**, **5c**, and **5d**, which exhibited the most potent inhibition of *E. coli* DNA gyrase, with the energy score ranging from −9.89 to −10.97 kcal/mol, while the other compounds **4b**, **4c**, and **5b** showed lower binding affinity with the energy score ranging from −8.66 to −8.80 kcal/mol.

By inspection of Figure 4, which describes the binding manner of the highly potent compounds **4a**, **5a**, **5c**, and **5d**, it was observed that the hydrazineyl derivative **4a** exhibited three additional H-bonds with the sidechain of **Asp73** (distance: 2.74, 3.08, and 3.16 Å, respectively). Moreover, the furanyl moiety displayed arene–cation interaction with key amino acid **Asn46**, which was not shown with the corresponding thienyl and pyridinyl moieties in the derivatives **4b** and **4c**. Furthermore, these moieties forced the hydrazineyl group away from binding with the essential amino acid **Asp73**. The formation of the formylpyrazole scaffold in the derivatives **5a**, **5c**, and **5d** gave the chance for good fitting through H-bonding or arene–cation interaction with **Asn46**.

According to the superimposition between the promising new compounds **4a**, **5a**, **5c**, and **5d** (Figure 5), the existence of the quinazolinone scaffold facilitated binding within the active site of *E. coli* DNA gyrase B through hydrophilic and hydrophobic interactions. Furthermore, incorporation with furanyl-hydrazone and formylpyrazole cores increased the chance for more fitting, and that could be a lead for the discovery of new *E. coli* DNA gyrase B inhibitors.

Table 4. Molecular docking results of the most active quinazolin-4(3*H*)one derivatives with *E. coli* DNA gyrase.

Compd.	Docking Score (Kcal/mol)	Amino Acid Residues (Bond Length A°)	Atoms of Compound	Type of Bond
Novobiocin	−10.25	Asn46(3.27); Asp73(1.91); Arg76	H(OH)(oxan-4-yl); H($OCONH_2$); C_6H_2(coumarin)	H-don H-don Arene–cation
4a	−10.48	Asn46; Asp73(3.08,3.16); Asp73(2.74); Gly77(2.63); Ile78	furan; NH(quinazolinone) NH(hydrazinyl) O(quinazolinone) Quinazolinone	Arene–cation H-don H-don H-acc Arene–cation
4b	−8.70	Gly77(2.66); Ile78	O(quinazolinone) Quinazolinone	H-acc Arene–cation
4c	−8.66	Gly77(2.83); Ile78	O(quinazolinone) Quinazolinone	H-acc Arene–cation
5a	−10.97	Asn46(2.53); Gly77(2.68); Ile78	O(CHO) O(quinazolinone) Quinazolinone	H-acc H-acc Arene–cation
5b	−8.80	Gly77(2.51); Ile78	O(quinazolinone) Quinazolinone	H-acc Arene–cation
5c	−9.89	Asn46; Ile78; Ile78	Pyrazole Pyrazole Quinazolinone	Arene–cation Arene–cation Arene–cation
5d	−10.74	Asn46(2.44); Asn46; Ile78; Ile78	O(CHO) 4-methoxyphenyl Pyrazole Quinazolinone	H-acc Arene–cation Arene–cation Arene–cation

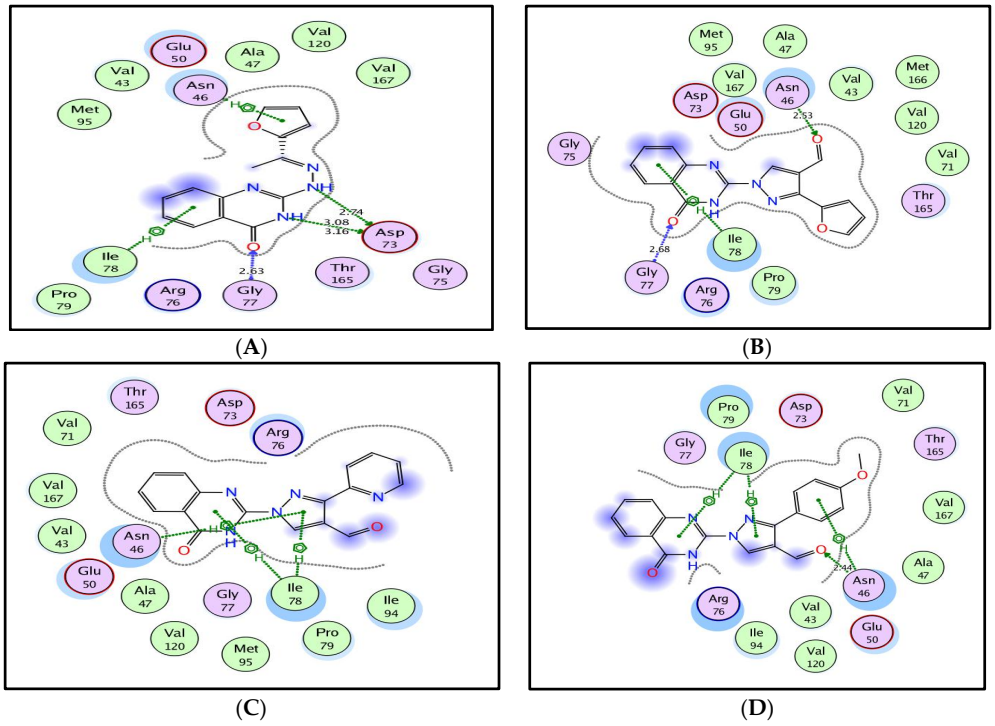

Figure 4. (**A**–**D**) Maps illustrate the 2D-binding poses of the promising quinazolinone targets, **4a**, **5a**, **5c**, and **5d** within the active site of *E. coli* DNA gyrase B (PDB code: 1AJ6).

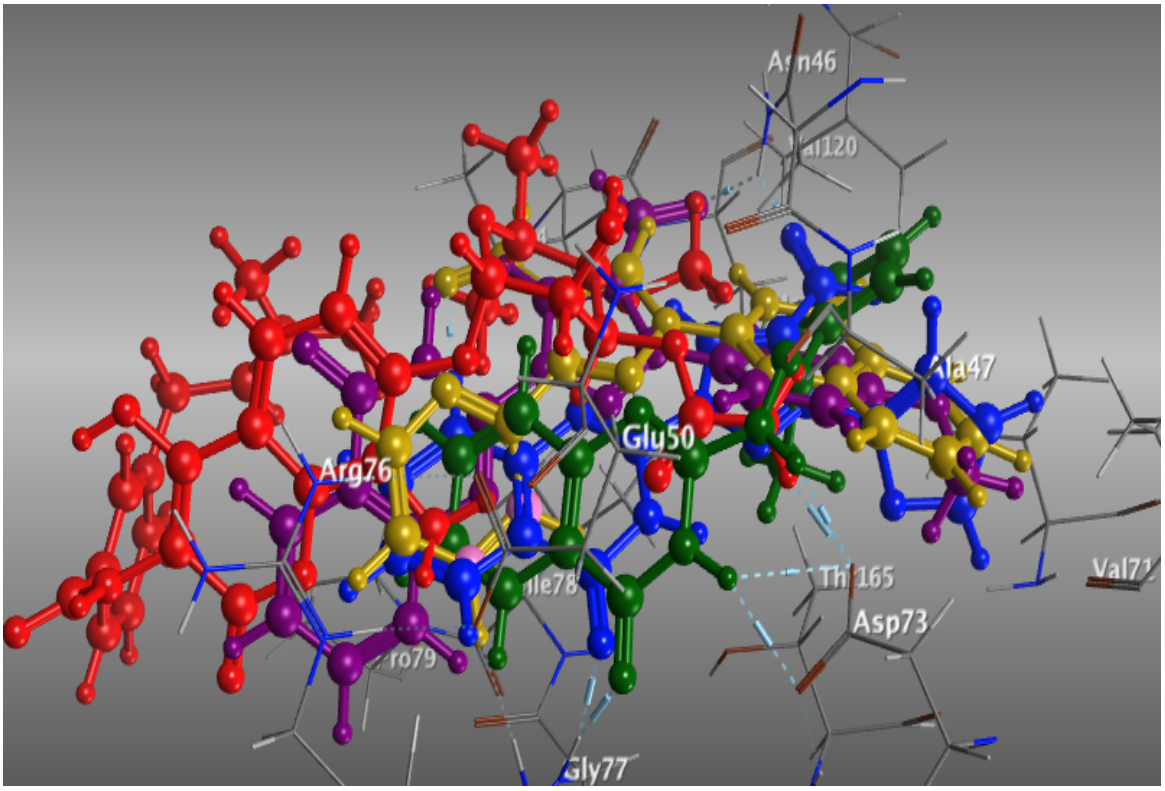

Figure 5. The 3D superimposition between the most potent compounds, **4a** (green), **5a** (blue), **5c** (yellow), and **5d** (purple), and the docked original ligand, Novobiocin (red), within the binding site of *E. coli* DNA gyrase B (PDB code: 1AJ6).

3.5. In Silico ADME Study

The study of absorption, distribution, metabolism, and excretion (ADME) for the designed targets is a key insight to obtain the optimal drug candidate. This prediction study was afforded using the free online tool, SwissADME. The optimum orally available drug obeys Lipinski's rule (molecule with MW $\leq$ 500, number of hydrogen bond donors $\leq$ 5, number of hydrogen bond acceptors $\leq$ 10, and MLogP $\leq$ 4.15) and Veber's rule (TPSA $\leq$ 140 Å^2, number of rotatable bonds $\leq$ 10). It was observed that all the assessed targets **4a**, **5a**, **5c**, and **5d** were compatible with the previous rules with no violations (Table 5). Concerning the bioavailability radar chart (Figure 6), it was noted that all compounds were located in the preferred range (pink area) corresponding to the five parameters lipophilicity (LIPO), flexibility (FLEX), solubility (INSOLU), polarity (POLAR), and SIZE, but kept away from the desirable area of saturation (INSATU), and that represented good prediction for their oral bioavailability.

Table 5. Predicted physicochemical properties of the most active quinazolin-4(3*H*)one derivatives **4a**, **5a**, **5c**, and **5d**.

Compd.	MW [1]	nHBD [2]	nHBA [3]	nRB [4]	MLogP [5]	TPSA (Å^2) [6]	Violations [7]
4a	268.27	2	4	3	1.58	83.28	0
5a	306.28	1	5	3	1.38	93.78	0
5c	317.30	1	5	3	1.58	93.53	0
5d	346.34	1	5	4	2.05	89.87	0

[1] Molecular weight; [2] number of hydrogen bond donor; [3] number of hydrogen bond acceptors; [4] number of rotatable bonds; [5] calculated lipophilicity (MLog Po/w); [6] topological polar surface area; [7] violations of the Lipinski and Veber rules.

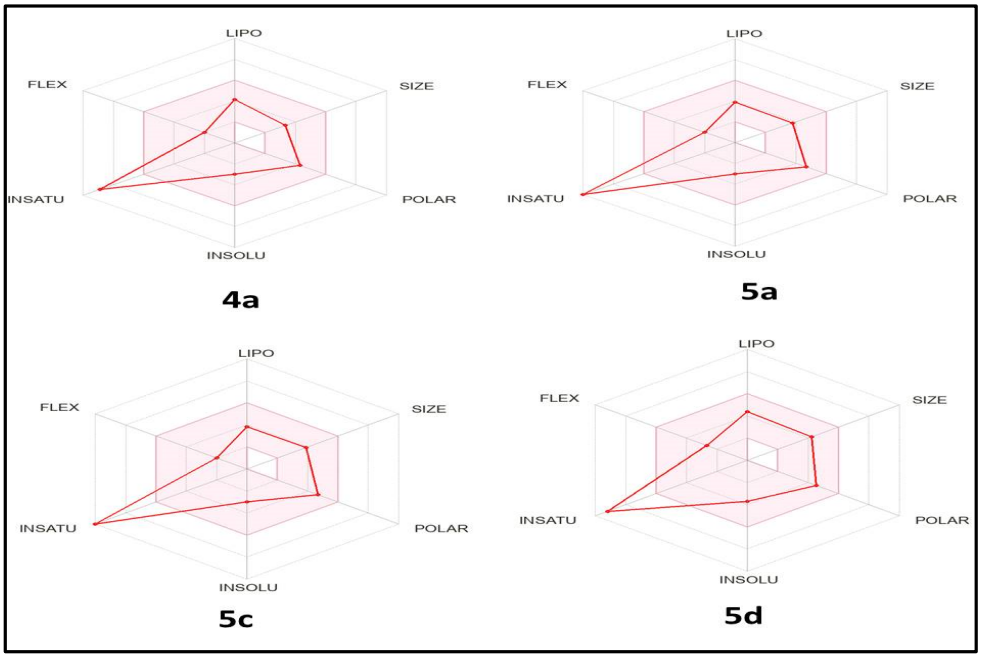

Figure 6. The bioavailability radar chart illustrating the oral bioavailability parameters of compounds **4a**, **5a**, **5c**, and **5d**.

The pharmacokinetic properties of the promising new quinazolin-4(3*H*)one derivatives **4a**, **5a**, **5c**, and **5d** were investigated and are depicted in Table 6 and Figure 7. All the derivatives revealed high expected gastrointestinal absorption with no BBB penetration, as they all inserted in the white region of the boiled-egg chart and away from the yellow one. Therefore, they were not predicted to cause CNS side effects and can be applied only for peripheral infections. It is known that p-glycoprotein (P-gp) is a drug efflux transporter and responsible for the pumping of drugs out of the cell, which could be one of the reasons for drug resistance. Through the SwissADME website, it was expected that all the screened compounds were not substrates for P-gp (red points, Figure 7), signifying a low chance of their efflux out of the cell with a maximum activity. Moreover, these derivatives exhibited high bioavailability scores of 0.55 with no PAIN alert.

Table 6. Predicted pharmacokinetic properties of the most active new quinazolin-4(3*H*)ones.

Comp. No.	GIT Absorption	BBB Permeability	P-gp Substrate	Bioavailability Score	PAINS Alert
4a	High	NO	NO	0.55	0
5a	High	NO	NO	0.55	0
5c	High	NO	NO	0.55	0
5d	High	NO	NO	0.55	0

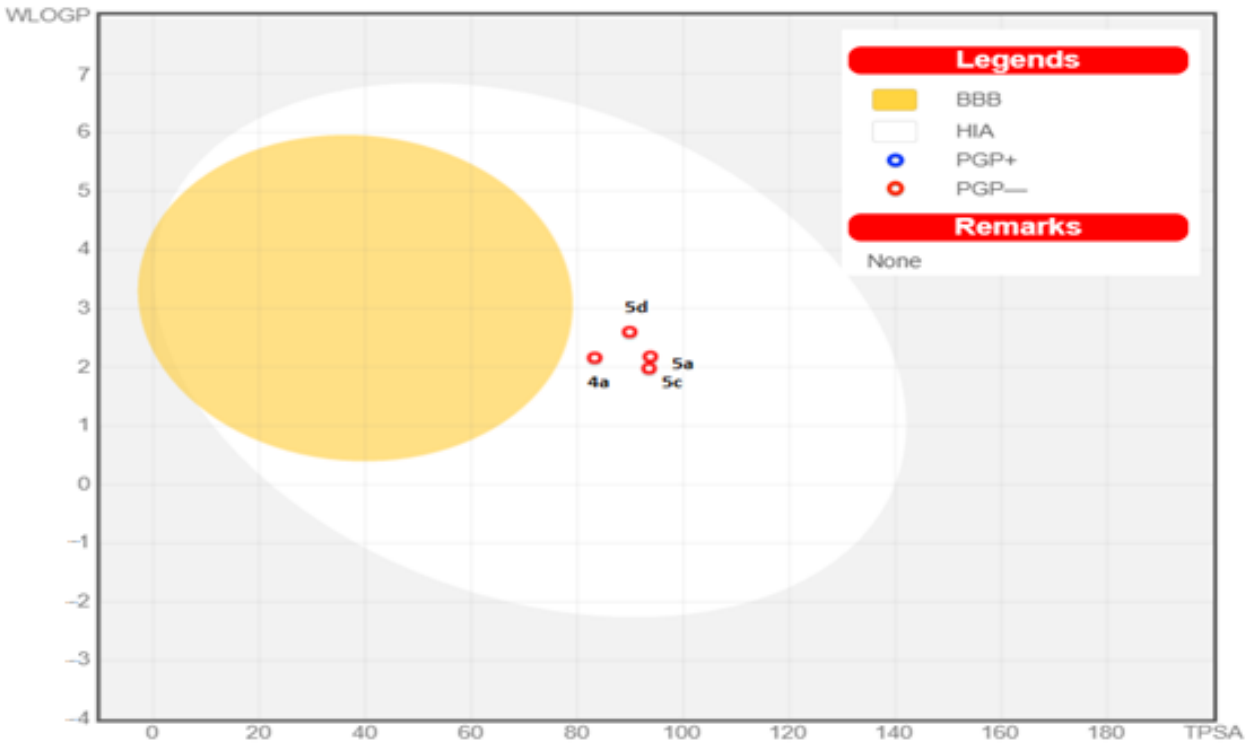

Figure 7. Boiled-egg chart illustrating the pharmacokinetic properties of the promising new quinazolin-4(3*H*)one derivatives.

4. Conclusions

The present study involved the design and synthesis of quinazolin-4(3*H*)-one derivatives (**4a**–**f**, **5a**–**d**) bearing hydrazone or formyl-pyrazole moieties as new antimicrobial agents targeting DNA gyraze enzyme. All the target quinazolin-4(3*H*)-one derivatives were evaluated for their in vitro antibacterial activities compared with Amoxicillin trihydrate against two Gram-positive bacteria and two Gram-negative bacteria. Furthermore, the target compounds were evaluated for their in vitro antifungal activities compared with Clotrimazole as the reference drug against two yeasts and two fungi. The new quinazolin-4(3*H*)-one derivatives showed significant antimicrobial activity compared with the reference drugs, especially the formyl-pyrazole derivatives. The 3-(Furan-2-yl)-1*H*-pyrazole-4-carbaldehyde derivative **5a** showed the most potent activity between the target compounds and the reference drugs with MIC values in the range of (1–16) µg/mL. In addition, the most active compounds (**4a**, **4b**, **4c**, **5a**, **5b**, **5c**, and **5d**) were evaluated for their inhibition activity against *E. coli* DNA gyrase compared with Novobiocin as the reference inhibitor. The results revealed that the most potent inhibition was achieved by **5a** with an IC_{50} value of 3.19 µM compared with Novobiocin with an IC_{50} value of 4.12 µM. Furthermore, the formyl pyrazole derivatives **5c** and **5d** showed potent inhibition activity of the target compounds with IC_{50} values of 4.09 and 3.51 µM, respectively. Moreover, the 2-(1-(furan-2-yl)ethylidene derivative **4a** was the most potent hydrazone derivative against DNA gyrase with an IC_{50} value of 4,17 µM, which sheds light on the role of the furanyl moiety in enhancing the antimicrobial activity and the DNA gyrase inhibitory activity. In addition, molecular docking studies were performed for the most active target quinazolin-4(3*H*)-one derivatives to predict their binding mode in the target *E. coli* DNA gyrase B active site. The results of the docking study were compatible with the DNA gyrase inhibitory activities, where the most binding affinity was obtained by the most potent inhibitors (**4a**, **5a**, **5c**, and **5d**) with the energy score range of (−9.89–−10.97) kcal/mol. Furthermore, ADME studies of the most active compounds predicted their good oral bioavailability.

The results gained from the present work revealed the significant antimicrobial activity of the target quinazolin-4(3*H*)-one compounds, especially compounds **4a**, **5a**, **5c**, and **5d**, as broad-spectrum antimicrobial agents targeting DNA gyrase enzyme.

Supplementary Materials: The following Supporting Information can be downloaded at: https://www.mdpi.com/article/10.3390/scipharm90030052/s1, Figures S1–S31: all the NMR spectra and some of the I.R and MS spectra of the new compounds; Figure S32: the 3D binding poses of compounds **4a**, **5a**, **5c**, and **5d** within the active site of *E. coli* DNA gyrase B; S33: in vitro antimicrobial assay; S34: in vitro DNA gyrase inhibitory assay; S35: molecular docking studies.

Author Contributions: Conceptualization, E.M.M.E.-D.; investigation, E.M.M.E.-D. and E.A.K.; methodology, E.M.M.E.-D. and E.A.K.; software, E.S.N.; writing—original draft preparation, E.M.M.E.-D. and E.S.N.; writing—review and editing, E.M.M.E.-D. All authors have read and agreed to the published version of the manuscript.

Funding: This research received no external funding.

Institutional Review Board Statement: Not applicable.

Informed Consent Statement: Not applicable.

Data Availability Statement: All data are mentioned in the manuscript.

Acknowledgments: The authors thank the National Research Centre for supporting this work.

Conflicts of Interest: The authors declare no conflict of interest.

References

1. Sifri, Z.C.; Chokshi, A.; Cennimo, D.; Horng, H. Global Contributors to Antibiotic Resistance. *J. Glob. Infect. Dis.* **2019**, *11*, 36–42. [CrossRef] [PubMed]
2. Lomazzi, M.; Moore, M.; Johnson, A.; Balasegaram, M.; Borisch, B. Antimicrobial resistance—Moving forward? *BMC Public Health* **2019**, *19*, 858. [CrossRef] [PubMed]
3. Li, B.; Webste, T.J. Bacteria antibiotic resistance: New challenges and opportunities for implant-associated orthopedic infections. *J. Orthop. Res.* **2018**, *36*, 22–32. [CrossRef] [PubMed]
4. Teitzel, G. Responding to Antimicrobial Resistance with Novel Therapeutics. *Trends Microbiol.* **2019**, *27*, 285–286. [CrossRef] [PubMed]
5. Egorov, A.M.; Ulyashova, M.M.; Rubtsova, M.Y. Bacterial Enzymes and Antibiotic Resistance. *Acta Naturae* **2018**, *10*, 33–48. [CrossRef] [PubMed]
6. Dubey, K.K.; Sharma, M. Reprogramming of antibiotics to combat antimicrobial resistance. *Arch. Pharm.* **2020**, *353*, e2000168. [CrossRef]
7. Klostermeier, D. Why Two? On the Role of (A-)Symmetry in Negative Supercoiling of DNA by Gyrase. *Int. J. Mol. Sci.* **2018**, *19*, 1489. [CrossRef]
8. Ma, Z.; Mduli, K. Mycobacterium tuberculosis DNA Gyrase as a Target for Drug Discovery. *Infect. Disord. Drug Targets* **2007**, *7*, 159–168. [CrossRef]
9. Annunziato, G. Strategies to Overcome Antimicrobial Resistance (AMR) Making Use of Non-Essential Target Inhibitors: A Review. *Int. J. Mol. Sci.* **2019**, *20*, 5844. [CrossRef]
10. Yi, L.; Lu, X. New Strategy on Antimicrobial-resistance: Inhibitors of DNA Replication Enzymes. *Curr. Med. Chem.* **2019**, *26*, 1761–1787. [CrossRef] [PubMed]
11. Yang, H.; Li, Q.; Su, M.; Luo, F.; Liu, Y.; Wang, D.; Fan, Y. Design, synthesis, and biological evaluation of novel 6-(pyridin-3-yl) quinazolin-4(3H)-one derivatives as potential anticancer agents via PI3K inhibition. *Bioorg. Med. Chem.* **2021**, *46*, 116346. [CrossRef] [PubMed]
12. Mirgany, T.O.; Abdalla, A.N.; Arifuzzaman, M.; Motiur Rahman, A.F.M.; Al-Salem, H.S. Quinazolin-4(3*H*)-one based potential multiple tyrosine kinase inhibitors with excellent cytotoxicity. *J. Enzyme Inhib Med. Chem.* **2021**, *36*, 2055–2067. [CrossRef] [PubMed]
13. Ramadan, S.K.; Elrazaz, E.Z.; Abouzid, K.A.M.; El-Naggar, A.M. Design, synthesis and in silico studies of new quinazolinone derivatives as antitumor PARP-1 inhibitors. *RSC Adv.* **2020**, *10*, 29475–29492. [CrossRef] [PubMed]
14. Masri, A.; Anwar, A.; Khan, N.A.; Shahbaz, M.S.; Khan, K.M.; Shahabuddin, S.; Siddiqui, R. Antibacterial Effects of Quinazolin-4(3*H*)-One Functionalized-Conjugated Silver Nanoparticles. *Antibiotics* **2019**, *8*, 179. [CrossRef] [PubMed]
15. Kavitha, K.; Mohan, S.; Srinivasan, N.; Suresh, R. Design, Synthesis, Characterization of Antimicrobial activity of Schiff bases of novel Quinazolin-4-one Derivatives. *Res. J. Pharm. Tech.* **2021**, *14*, 466–470. [CrossRef]
16. Demirel, U.U.; Yilmaz, A.; Türkdağı, H.; Öztürk, B.; Arslan, U. Investigation of Some 3*H*-Quinazolin-4-One Derivatives in Vitro Antimicrobial Effect and Cytotoxicity on Human Gingival Fibroblasts. *Polycycl. Aromat. Compd.* **2021**, *41*, 1623–1630. [CrossRef]

17. Thorat, D.B.; Shivkumar, B.; Rao, N.; Mohankumar, K.M. Synthesis and Evaluation of new 4(3*H*)-quinazolinones derivatives as potential Anti-Inflammatory agents. *Asian J. Pharm. Sci.* **2021**, *11*, 213–218. [CrossRef]
18. Kumar, S.; Aghara, J.C.; Alex, A.T.; Aranjani, J.M.; Joesph, A. Novel Quinolone Substituted Quinazolin-4(3*H*)-Ones as Anti-Inflammatory, Anticancer Agents: Synthesis and Biological Screening. *Indian J. Pharm. Educ. Res.* **2018**, *52*, S268–S276. [CrossRef]
19. Ayyad, R.A.; Sakr, H.M.; El-Gamal, K.M. Design, Synthesis, Computer Modeling and Analgesic Activity of Some New Disubstituted Quinazolin-4(3*H*)-ones. *Med. Chem.* **2016**, *6*, 299–305. [CrossRef]
20. Osarumwense, P.; Edema, M.; Usifoh, C. Synthesis and Anagesic activities of Quinazolin-4(3*H*)-One, 2-Methyl-4(3*H*)-Quinazolinone and 2–Phenyl-4(3*H*)-quinazolin-4(3*H*)–one. *J. Drug Deliv. Ther.* **2020**, *10*, 87–91. [CrossRef]
21. Birhan, Y.S.; Bekhit, A.A.; Hymete, A. In vivo antimalarial evaluation of some 2,3-disubstituted-4(3*H*)-quinazolinone derivatives. *BMC Res. Notes* **2015**, *8*, 589. [CrossRef]
22. Bule, M.H.; Haymete, A.; Kefale, B. Synthesis and In-Vivo Pharmacological Evaluation of Some Novel 4(3*H*)- Quinazolinone Derivatives as Potential Anti-malarial Agents. *Drug. Des.* **2015**, *4*, 121. [CrossRef]
23. Chen, L.; Wang, X.; Tang, X.; Xia, R.; Guo, T.; Zhang, C.; Li, X.; Xue, W. Design, synthesis, antiviral bioactivities and interaction mechanisms of penta-1,4-diene-3-one oxime ether derivatives containing a quinazolin-4(3*H*)-one scaffold. *BMC Chem.* **2019**, *13*, 34. [CrossRef]
24. Tran, T.P.; Ellsworth, E.L.; Sanchez, J.P.; Watson, B.M.; Stier, M.A.; Showalter, H.D.H.; Domagala, J.M.; Shapiro, M.A.; Joannides, E.T.; Gracheck, S.J.; et al. Structure–activity relationships of 3-aminoquinazolinediones, a new class of bacterial type-2 topoisomerase (DNA gyrase and topo IV) inhibitors. *Bioorg. Med. Chem. Lett.* **2007**, *17*, 1312. [CrossRef]
25. Ghorab, M.M.; Alqahtani, A.S.; Soliman, A.M.; Askar, A.A. Novel *N*-(Substituted) Thioacetamide Quinazolinone Benzenesulfonamides as Antimicrobial Agents. *Int. J. Nanomed.* **2020**, *15*, 3161–3180. [CrossRef]
26. Xue, W.; Wang, Y.; Lian, X.; Li, X.; Pang, J.; Kirchmair, J.; Wu, K.; Han, Z.; You, X.; Zhang, H.; et al. Discovery of *N*-quinazolinone-4-hydroxy-2-quinolone-3-carboxamides as DNA gyrase B-targeted antibacterial agents. *J. Enzyme Inhib. Med. Chem.* **2022**, *37*, 1620–1631. [CrossRef]
27. Verma, G.; Marella, A.; Shaquiquzzaman, M.; Akhtar, M.; Ali, M.R.; Alam, M.M. A review exploring biological activities of hydrazones. *J. Pharm. Bioallied Sci.* **2014**, *6*, 69–80. [CrossRef]
28. Rollas, S.; Küçükgüzel, S.G. Biological Activities of Hydrazone Derivatives. *Molecules* **2007**, *12*, 1910–1939. [CrossRef]
29. Ansari, A.; Ali, A.; Asif, A. Shamsuzzman Review: Biologically active pyrazole derivatives. *New J. Chem.* **2017**, *41*, 16–41. [CrossRef]
30. Karrouchi, K.; Radi, S.; Ramli, Y.; Taoufik, J.; Mabkhot, Y.N.; Al-aizari, F.A.; Ansar, M. Synthesis and Pharmacological Activities of Pyrazole Derivatives: A Review. *Molecules* **2018**, *23*, 134. [CrossRef]
31. Sridhar, P.; Alagumuthu, M.; Arumugam, S.; Reddy, S.R. Synthesis of quinoline acetohydrazide-hydrazone derivatives evaluated as DNA gyrase inhibitors and potent antimicrobial agents. *RSC Adv.* **2016**, *6*, 64460–64468. [CrossRef]
32. Ragab, A.; Elsisi, D.M.; Abu Ali, O.A.; Abusaif, M.S.; Askar, A.A.; Farag, A.A.; Ammar, Y.A. Design, synthesis of new novel quinoxalin-2(1*H*)-one derivatives incorporating hydrazone, hydrazine, and pyrazole moieties as antimicrobial potential with in-silico ADME and molecular docking simulation. *Arab. J. Chem.* **2022**, *15*, 103497. [CrossRef]
33. Hassan, A.S.; Askar, A.A.; Naglah, A.M.; Almehizia, A.A.; Ragab, A. Discovery of New Schiff Bases Tethered Pyrazole Moiety: Design, Synthesis, Biological Evaluation, and Molecular Docking Study as Dual Targeting DHFR/DNA Gyrase Inhibitors with Immunomodulatory Activity. *Molecules* **2020**, *25*, 2593. [CrossRef]
34. Sun, J.; Lv, P.C.; Yin, Y.; Yuan, R.J.; Ma, J.; Zhu, H.L. Synthesis, structure and antibacterial activity of potent DNA gyrase inhibitors: *N*′-benzoyl-3-(4-bromophenyl)-1*H*-pyrazole-5-carbohydrazide derivatives. *PLoS ONE* **2013**, *8*, e69751. [CrossRef]
35. Viegas-Junior, C.; Danuello, A.; da Silva Bolzani, V.; Barreiro, E.J.; Fraga, C.A. Molecular hybridization: A useful tool in the design of new drug prototypes. *Curr. Med. Chem.* **2007**, *14*, 1829–1852. [CrossRef] [PubMed]
36. Sree, B.S.; Rao, A.L.; Babu, P.S.; Kiran, K.S.; Vandana, K. Synthesis and antimicrobial screening of some novel quinazolinones and its derivatives. *Indian J. Pharm. Pharmacol.* **2017**, *4*, 130–133. [CrossRef]
37. Gruner, M.; Rehwald, M.; Katrin Eckert, K.; Gewald, K. New Syntheses of 2-Alkylthio-4-Oxo-3,4-Dihydroquinazolines, 2-Alkylthioquinazolines, as Well as Their Hetero Analogues. *Heterocycles* **2000**, *53*, 2363–2377. [CrossRef]
38. Penna, C.A.; Marino, S.G.; Gutkind, G.O.; Clavin, M.; Ferraro, G.; Martino, V. Antimicrobial activity of Eupatorium species growing in Argentina. *J. Herbs Spices Med. Plants* **1988**, *5*, 21–28. [CrossRef]
39. Wiegand, I.; Hilpert, K.; Hancock, R.E. Agar and broth dilution methods to determine the minimal inhibitory concentration (MIC) of antimicrobial substances. *Nat. Protoc.* **2008**, *3*, 163–175. [CrossRef]
40. Phillips, J.W.; Goetz, M.A.; Smith, S.K.; Zink, D.L.; Polishook, J.; Onishi, R.; Salowe, S.; Wiltsie, J.; Allocco, J.; Sigmund, J.; et al. Discovery of Kibdelomycin, A Potent New Class of Bacterial Type II Topoisomerase Inhibitor by Chemical-Genetic Profiling in Staphylococcus aureus. *Chem. Biol.* **2011**, *18*, 955–965. [CrossRef]
41. Maxwell, A.; Burton, N.P.; O'Hagan, N. High-throughput assays for DNA gyrase and other topoisomerases. *Nucleic Acids Res.* **2006**, *34*, e104. [CrossRef]
42. Mohi El-Deen, E.M.; Abd El-Meguid, E.A.; Karam, E.A.; Nossier, E.S.; Ahmed, M.F. Synthesis and Biological Evaluation of New Pyridothienopyrimidine Derivatives as Antibacterial Agents and *Escherichia coli* Topoisomerase II Inhibitors. *Antibiotics* **2020**, *9*, 695. [CrossRef]

43. Hashem, H.E.; Amr, A.E.G.E.; Nossier, E.S.; Elsayed, E.A.; Azmy, E.M. Synthesis, antimicrobial activity and molecular docking of novel thiourea derivatives tagged with thiadiazole, imidazole and triazine moieties as potential DNA gyrase and topoisomerase IV inhibitors. *Molecules* **2020**, *25*, 2766. [CrossRef]
44. Mohi El-Deen, E.M.; El-Meguid, E.A.A.; Hasabelnaby, S.; Karam, E.A.; Nossier, E.S.; El-Deen, E.M.; El-Meguid, E.A.A. Synthesis, Docking Studies, and In Vitro Evaluation of Some Novel Thienopyridines and Fused Thienopyridine-Quinolines as Antibacterial Agents and DNA Gyrase Inhibitors. *Molecules* **2019**, *24*, 3650. [CrossRef]
45. Daina, A.; Michielin, O.; Zoete, V. SwissADME: A free web tool to evaluate pharmacokinetics, drug-likeness and medicinal chemistry friendliness of small molecules. *Sci. Rep.* **2017**, *7*, 42717. [CrossRef]
46. Othman, I.M.; Alamshany, Z.M.; Tashkandi, N.Y.; Gad-Elkareem, M.A.; Anwar, M.M.; Nossier, E.S. New pyrimidine and pyrazole-based compounds as potential EGFR inhibitors: Synthesis, anticancer, antimicrobial evaluation and computational studies. *Bioorg. Chem.* **2021**, *114*, 105078. [CrossRef]
47. Mohi El-Deen, E.M.; Anwar, M.M.; Abd El-Gwaad, A.A.; Karam, E.A.; El-Ashrey, M.K.; Kassab, R.R. Design and synthesis of some novel pyridothienopyrimidine derivatives and their biological evaluation as antimicrobial and anticancer agents targeting EGFR enzyme. *Arab. J. Chem.* **2022**, *15*, 103751. [CrossRef]
48. El-Tombary, A.A.; Ismail, K.A.; Aboulwafa, O.M.; Omar, A.M.M.; El-Azzouni, M.Z.; El-Mansoury, S.T. Novel triazolo [4, 3-a] quinazolinone and bis-triazolo [4, 3-a: 4, 3′-c] quinazolines: Synthesis and antitoxoplasmosis effect. *Farmaco* **1999**, *54*, 486–495. [CrossRef]
49. Rafeeq, M.; Reddy, B.S.; Reddy, C.V.R.; Naidu, A.; Dubey, P.K. Green and efficient synthesis of 2-(4-oxo-3, 4-dihydroquinazolin-2-yl)-2, 3-dihydropthalazine-1, 4-dione. *Indian J. Chem.* **2015**, *54B*, 412–417. [CrossRef]
50. Singh, K.; Ralhan, S.; Sharma, P.K.; Dhawan, S.N. Vilsmeier–Haack Reaction on Hydrazones: A Convenient Synthesis of 4-formylpyrazoles. *J. Chem. Res.* **2005**, *2005*, 316–318. [CrossRef]